Electronic Supplementary Material (ESI) for Analyst.


# Supporting Information

# Template-free assembly of Cu,N-codoped hollow carbon nanospheres as low-cost and highly efficient peroxidase nanozymes

Xian-Sen Tao[a], Yuan Liu[c], Ying Gan[a], Yue-Tong Li[a], Jingquan Sha*[a], An-Min Cao[b]

[a] The talent culturing plan for leading disciplines of Shandong Province, School of Chemistry, Chemical Engineering and Materials, Jining University, Qufu, Shandong, 273155, P.R China.

[b] CAS Key Laboratory of Molecular Nanostructure and Nanotechnology, and Beijing National Laboratory for Molecular Sciences, Institute of Chemistry,Chinese Academy of Sciences (CAS), Beijing 100190, China.

[c] Nanozyme Medical Center, School of Basic Medical Sciences, Zhengzhou University, Zhengzhou 450001, China.

*Corresponding author: E-mail address: shajq2002@126.com

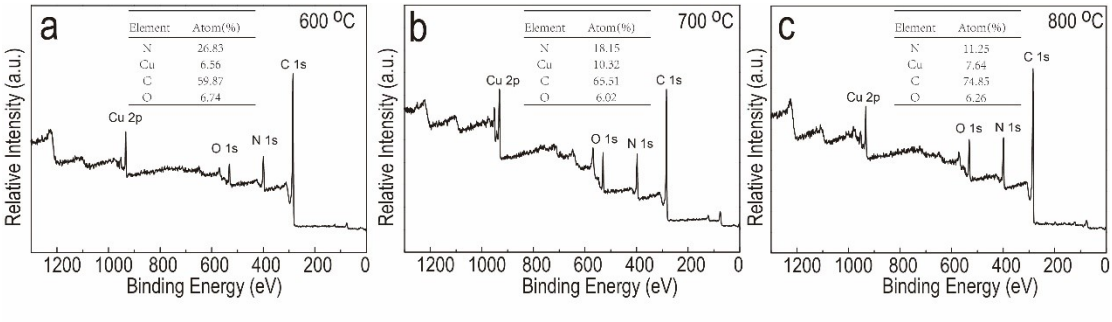


**Fig. S1.** XPS survey scans of CuNHCN calcinated at 600°C, 700 °C and 800 °C. Insets: contents of C, N, O and Cu.

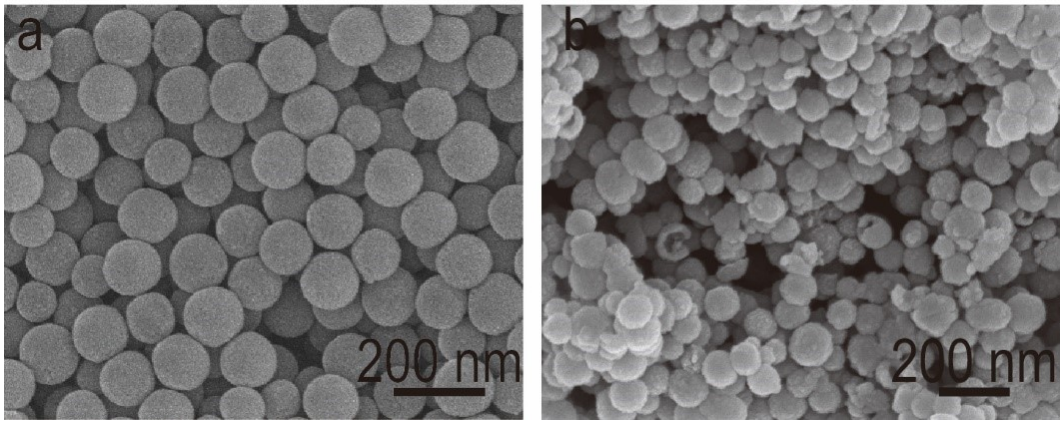


**Fig. S2.** SEM images of the (a) hollow Cu-PmPD nanospheres and (b) CuNHCN.

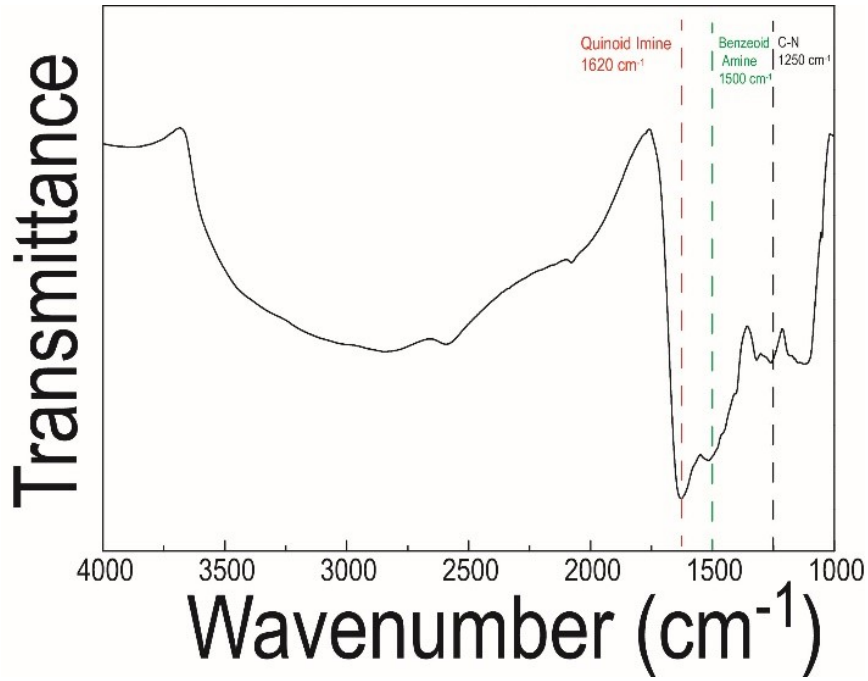


**Fig. S3.** FT-IR spectrum of the hollow Cu-PmPD nanospheres

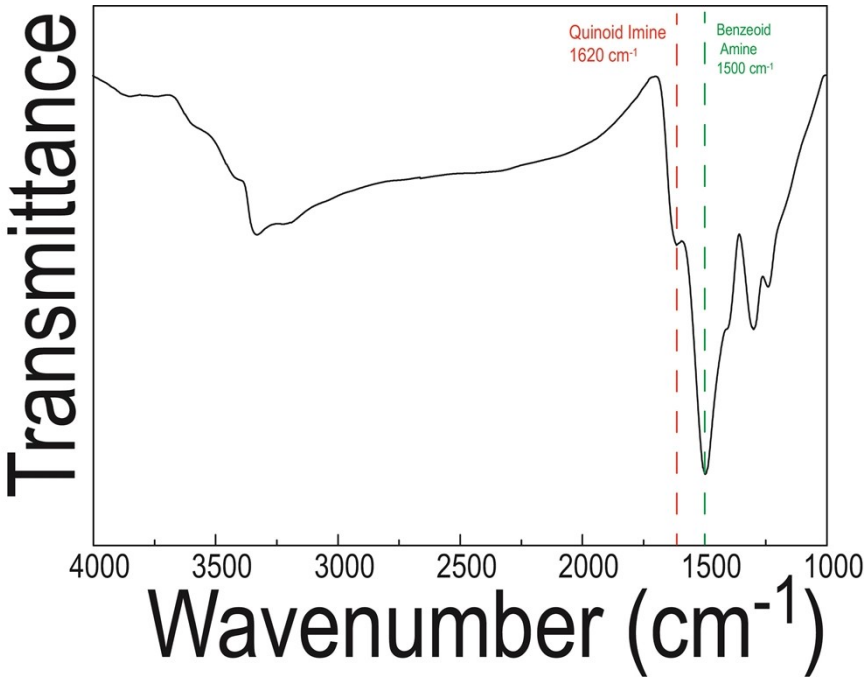


**Fig. S4.** FT-IR spectrum of the interior parts of the Cu-PmPD nanospheres (the interior parts was obtained according to the literature[1,2]. Briefly, the interior parts was dissolved in the reaction solvent, which could be obtained through centrifugation and freeze drying)

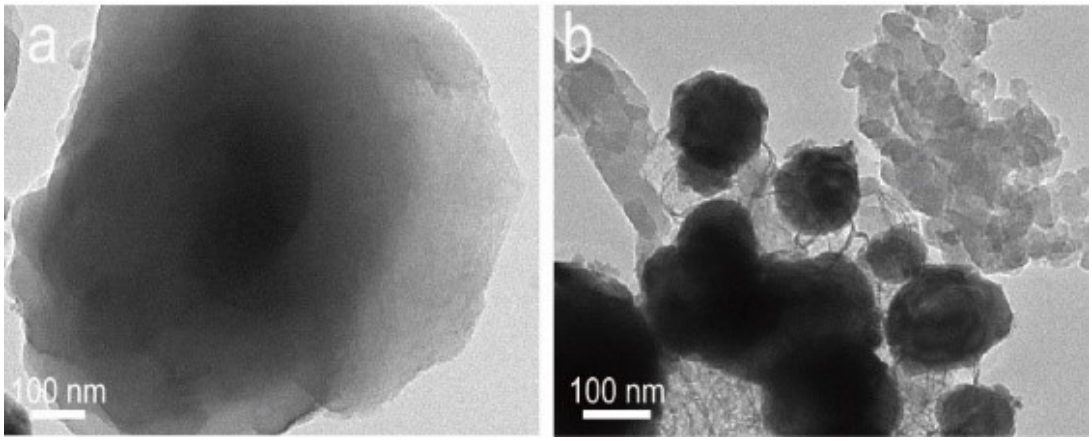


**Fig. S5.** TEM images of the (a) NC and (b)CuN

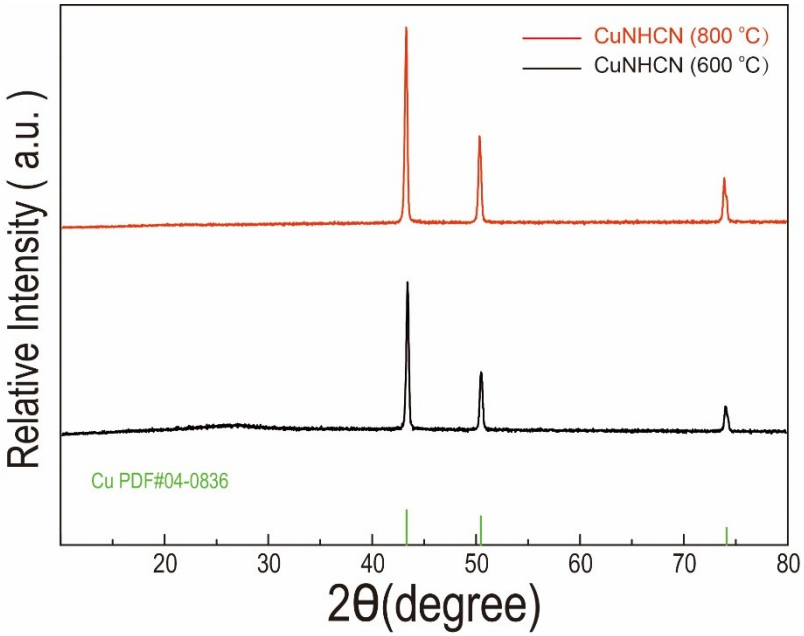


**Fig. S6.** $N_2$ adsorption-desorption isotherm curves and pore size distribution curves of (a) CuC,(b) NC, (c) CuNHCN.

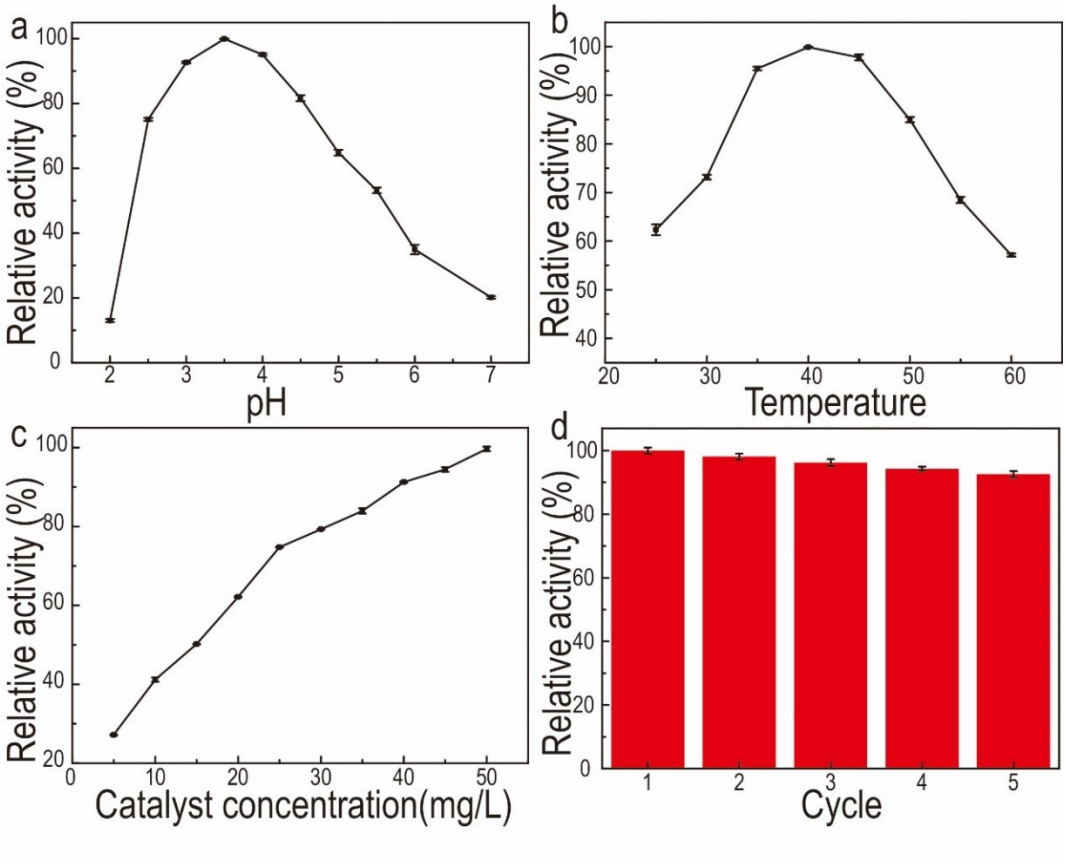


**Fig. S7.** Effects of (a) pH, (b) temperature, (c) concentration and (d) stability of CuNHCN under optimized reaction conditions. Error bar shows the standard deviation of three independent measurements.

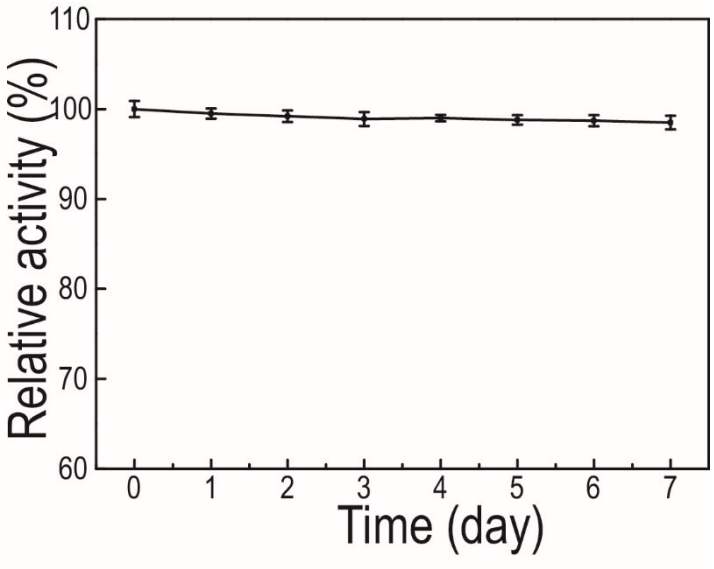


**Fig. S8** The storage performance of CuNHCN under optimized reaction conditions

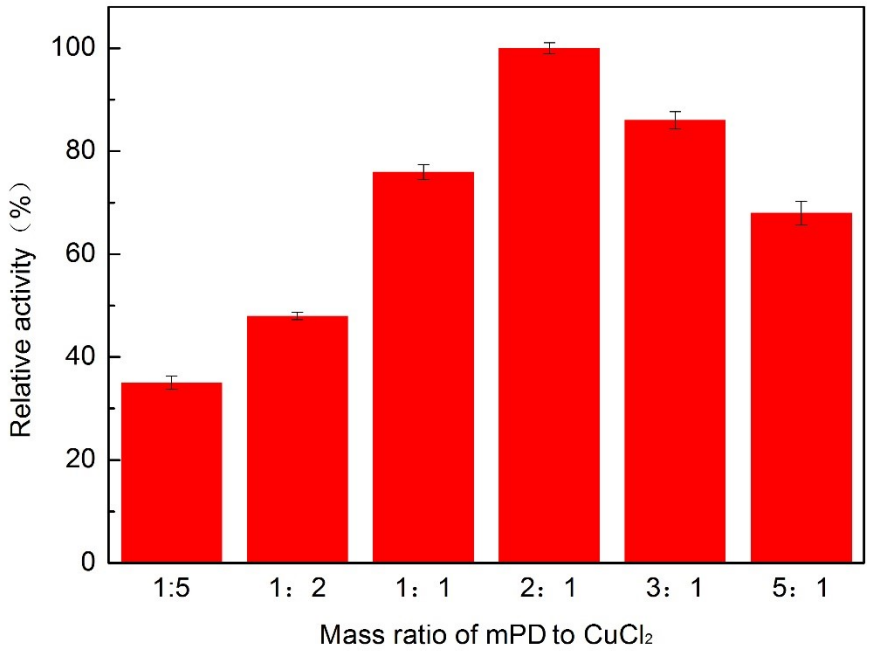


**Fig.S9.** Influence of the mass ratio of mPD to $CuCl_2$ on the peroxidase-like catalytic performance

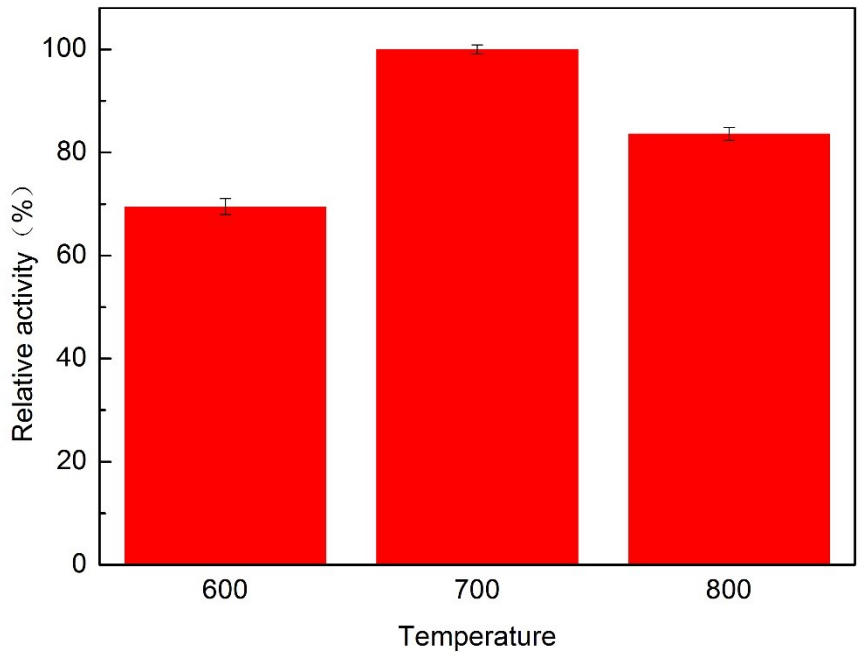


**Fig.S10.** Influence of the temperature on the peroxidase-like catalytic performance of CuNHCN

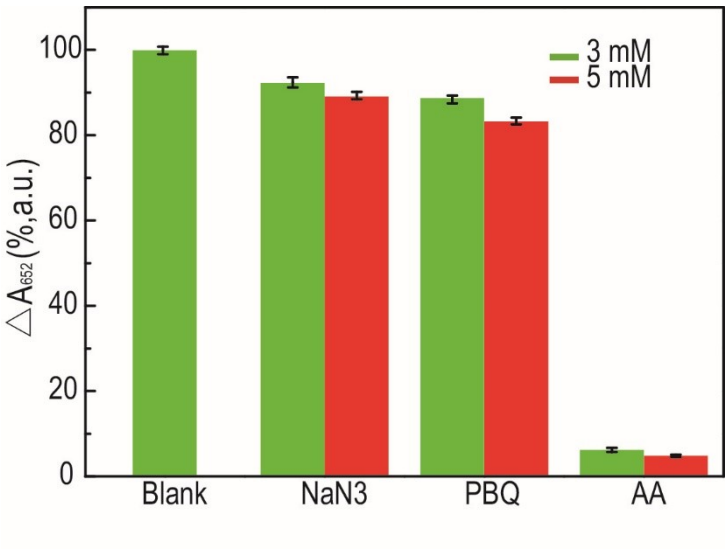


**Fig. S11.** The influence of different concentrations of ROS scavengers ($NaN_3$, PBQ and AA) on the $A_{652}$ of the CuNHCN/TMB/$H_2O_2$ system. Reaction condition: 0.15 mM TMB, 0.1 mM $H_2O_2$, 25 mg $L^{-1}$ catalyst, pH 3.5 acetate buffer(0.2 M), 4 min reaction at 40 ◦C.

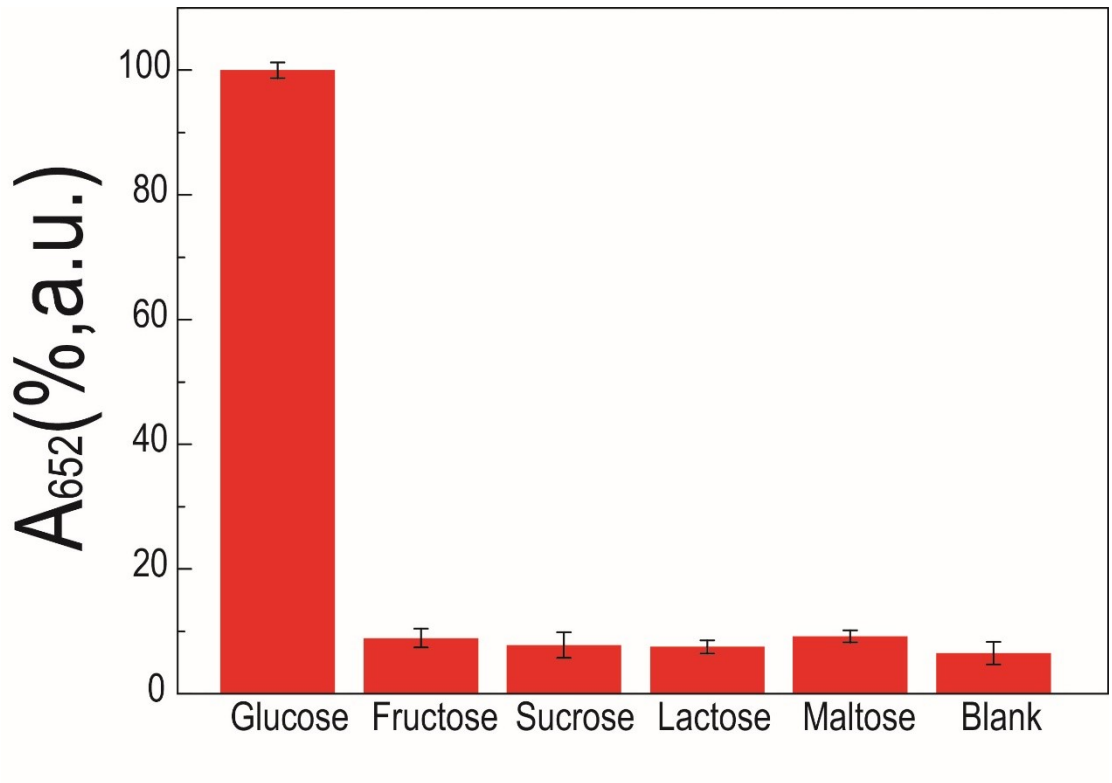


**Fig. S12.** The influence of different substrates (5 mM fructose, 5 mM sucrose, 5 mM lactose, 5 mM Maltose or 0.5 mM glucose) on the $A_{652}$ of the glucose oxidase/TMB/CuNHCN system. Error bar shows the standard deviation of three independent measurements.

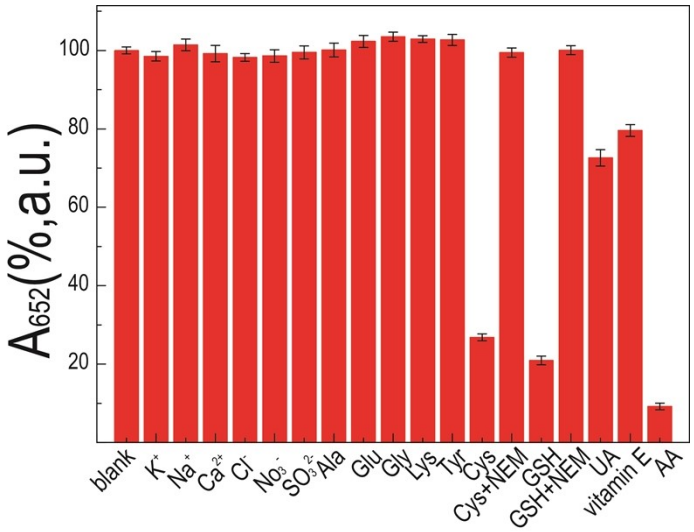


**Fig. S13.** The influence of different substrates (metal ion($K^+$, $Na^+$,$Ca^{2+}$) (5 mM), sulfite (5 mM) , nitrite (0.5 mM), chloride(0.5 mM), alanine (Ala) (5 mM), glutamic acid (Glu) (5 mM), glycine (Gly) (5 mM), lysine (Lys) (5 mM), tyrosine (Tyr) (5 mM),Cysteine (Cys) (0.5 mM), glutathione (GSH) (0.5 mM), Cys+NEM, GSH+NEM, uric acid (UA) (0.5 mM), vitamin E (0.5 mM) and AA (0.5 mM)) on the $A_{652}$ of the $H_2O_2$/TMB/CuNHCN system. Error bar shows the standard deviation of three independent measurements.

**Table S1** Comparison of the CuNHCN based on colorimetry method for the determination of glucose and AA.

| Material | $K_m$ (mM) | | $V_{max}$ ($10^{-8}$ M/s) | | Refs |
|---|---|---|---|---|---|
| | TMB | $H_2O_2$ | TMB | $H_2O_2$ | |
| Au NPs /Graphene- | 0.38 | 26.4 | 18.3 | 15.41 | [3] |
| Au NPs/PVP-GNs | 2.63 | 104 | 13.04 | 11.98 | [3] |
| Cu/Au/Pt TNPs | 0.15 | 2.34 | 7.33 | 136.5 | [4] |
| β-CD-Cu-NCs | 0.543 | 32.87 | 43.4 | 45.2 | [4] |
| Hollow CuS nanocubes | 1.62 | 0.94 | 16.64 | 2.55 | [6] |
| Au loaded nanoporous $Fe_2O_3$ nanozymes | 0.049 | 138.5 | 5.882 | 4.770 | [7] |
| Pt hollow nanodendrites | 0.81 | 6.9 | 1.2 | 9.9 | [8] |
| $Fe_3O$ with aptamer | 0.088 | 30.24 | 0.406 | 0.342 | [9] |
| Au-Ni/g-$C_3N4$ | 0.16 | 4.47 | 2.34 | 6.16 | [10] |
| $Co_3O_4$ nanocrystals | 0.49 | 1.90 | 16 | 12.7 | [11] |
| HRP | 0.434 | 3.70 | 10.0 | 8.71 | [12] |
| CuNHCN | 0.0655 | 0.918 | 5.85 | 42.84 | This work |

**Reference**


[1] D.-S. Bin, Z.-X. Chi, Y. Li, K. Zhang, X. Yang, Y.-G. Sun, J.-Y. Piao, A.-M. Cao and L.-J. Wan, *J. Am. Chem. Soc.*, 2017, **139**, 13492–13498.

[2] X.-S. Tao, Y.-G. Sun, Y. Liu, B.-B. Chang, C.-T. Liu, Y.-S. Xu, X.-C. Yang and A.-M. Cao, *ACS Appl. Mater. Interfaces*, 2020, **12**, 13182–13188.

[3] X. Chen, X. Tian, B. Su, Z. Huang, X. Chen and M. Oyama, *Dalton Trans*., 2014, 43, 7449–7454.

[4] P. Wu, P. Ding, X. Ye, L. Li, X. He and K. Wang, *RSC Adv.*, 2019, 9, 14982–14989.

[5] Y. Zhong, C. Deng, Y. He, Y. Ge and G. Song, *Microchim. Acta*, 2016, 183, 2823–2830.

[6] J. Zhu, X. Peng, W. Nie, Y. Wang, J. Gao, W. Wen, J. N. Selvaraj, X. Zhang and S. Wang, *Biosens. Bioelectron*., 2019, 141, 111450.

[7] K. Boriachek, M. K. Masud, C. Palma, H.-P. Phan, Y. Yamauchi, Md. S. A. Hossain, N.-T. Nguyen, C. Salomon and M. J. A. Shiddiky, *Anal. Chem.*, 2019, 91, 3827–3834.

[8] C. Ge, R. Wu, Y. Chong, G. Fang, X. Jiang, Y. Pan, C. Chen and J.-J. Yin, *Adv. Funct. Mater*., 2018, 28, 1801484.

[9] S. Li, X. Zhao, X. Yu, Y. Wan, M. Yin, W. Zhang, B. Cao and H. Wang, *Anal. Chem*., 2019, 91, 14737–14742.

[10] G. Darabdhara, J. Bordoloi, P. Manna and M. R. Das, *Sens. Actuators B Chem*., 2019, 285, 277–290.

[11] W. Li, J. Wang, J. Zhu and Y.-Q. Zheng, *J. Mater. Chem. B*, 2018, 6, 6858–6864.
[12] J. Wu, X. Wang, Q. Wang, Z. Lou, S. Li, Y. Zhu, L. Qin and H. Wei, *Chem. Soc. Rev.*, 2019, 48, 1004–1076.